

University of Arkansas, Fayetteville

ScholarWorks@UARK

Chemical Engineering Undergraduate Honors
Theses

Chemical Engineering

5-2022

Quantification of Slit-Like Pores Through Using Liquid Crystals as a Template

Dominique Savage

University of Arkansas, Fayetteville

Follow this and additional works at: <https://scholarworks.uark.edu/cheguht>



Part of the [Membrane Science Commons](#), [Polymer Science Commons](#), and the [Service Learning Commons](#)

Citation

Savage, D. (2022). Quantification of Slit-Like Pores Through Using Liquid Crystals as a Template. *Chemical Engineering Undergraduate Honors Theses* Retrieved from <https://scholarworks.uark.edu/cheguht/182>

This Thesis is brought to you for free and open access by the Chemical Engineering at ScholarWorks@UARK. It has been accepted for inclusion in Chemical Engineering Undergraduate Honors Theses by an authorized administrator of ScholarWorks@UARK. For more information, please contact scholar@uark.edu, uarepos@uark.edu.

Quantification of Slit-Like Pores Through Using Liquid Crystals as a Template

By: Dominique Savage

Thesis Lab Partner: Isaac Hopwood

Graduate Student Assistance: Homa Ghaiedi and Jude Obijiaku

Thesis Advisor: Dr. Karthik Nayani

Ralph E. Martin Department of Chemical Engineering

University of Arkansas

Fayetteville, AR

April 29th, 2022

Introduction

The purpose of this research is to manufacture a membrane with slit-like pores to achieve particle filtration. Slit-like pore membranes are preferred over conventional membranes with cylindrical pores since slit-like pores have two length scales that can be manipulated to better control cut off and flux through the membrane. This project focuses on manufacturing slit-like pore membranes through the use of two liquid crystals, 1,4-bis[4-(6-acryloyloxyhexyloxy)benzoyloxy]-2-methylbenzene (RM257) and 4-Cyano-4'-pentylbiphenyl (5CB). This method for making slit-like pores has not been widely investigated nor has the morphology of the membrane pores and mechanical properties of such a membrane been addressed.

Background

Liquid crystals (LCs) have a variety of applications for development of soft materials, photovoltaics, sensors, and visual displays [1], [2]. LCs can exist in either a crystalline solid, nematic, or isotropic liquid phase as displayed in Figure 1 [3]. Since LCs are thermotropic, temperature alone determines the phase of the LC [1]. When in the nematic phase, LCs exhibit anisotropic properties of crystalline solids and fluid properties of isotropic liquids [2]. LCs in the nematic phase can retain long-range orientational order in at least one direction while being able to diffuse through translation and rotation motion at liquid comparable rates [4]. For 1,4-bis[4-(6-acryloyloxyhexyloxy)benzoyloxy]-2-methylbenzene (RM257) the crystalline to nematic transition occurs at 70 °C and the nematic to isotropic transition occurs at 126 °C [5]. For 4-Cyano-4'-pentylbiphenyl (5CB) the crystalline to nematic transition occurs at 22 °C and the nematic to isotropic transition occurs at 35.5 °C [1]. The molecular structures for RM257 and 5CB are shown in Figure 2 [2].

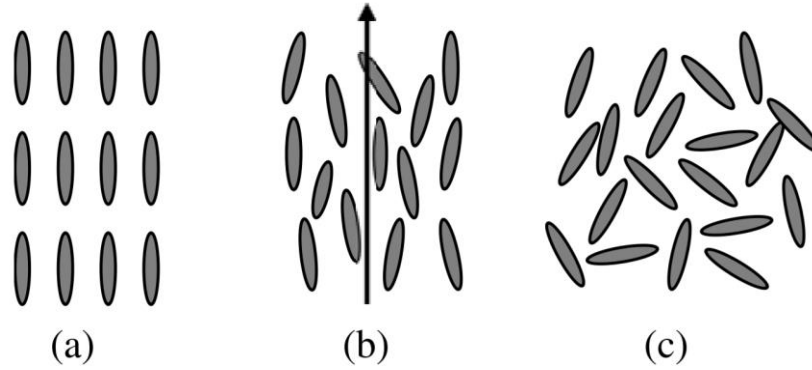


Figure 1. LC molecules in (a) crystalline, (b) nematic and (c) isotropic phases [4]

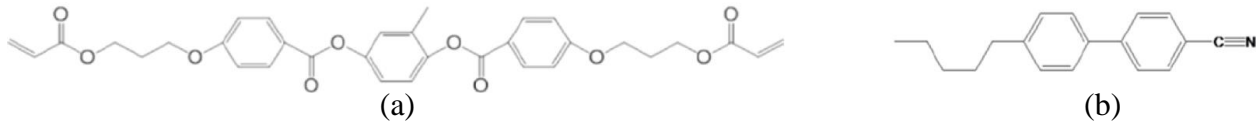


Figure 2. (a) RM 257 and (b) 5CB [2]

5CB is one of the most studied LCs and has a wide range of applications due to its physical ability to have weak UV-Visible absorption, optical anisotropy, chemical stability, among other traits [1]. It has been reported that RM257/5CB mixtures are completely miscible in the nematic state for high concentrations of 5CB [6]. Karausta and Bukusoglu outlined a method for manufacturing LC membranes using a RM257/5CB mixture which was used as a reference for this research [2]. RM257 is the reactive monomer and 5CB is the non-reactive monomer in a mixture [2]. The LC mixture can be cured through use of UV light which initiates RM257 crosslinking to form the solid membrane [2]. 5CB can then be extracted using ethanol solution [2]. When the 5CB is removed, it creates pores in the membrane. Once the membrane is removed from the ethanol solution, it shrinks [2]. Figure 3 illustrates the polymerization, extraction, and shrinkage process.

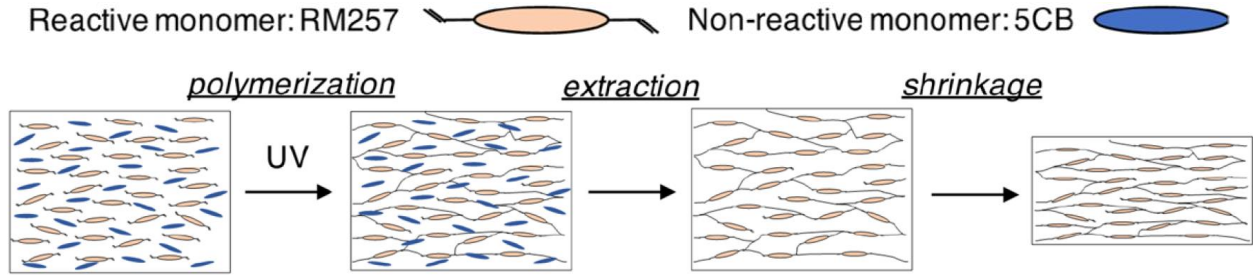


Figure 3. Procedure of membrane RM257 polymerization and 5CB extraction [2]

Membranes are a useful technology for a variety of applications including N₂ and O₂ separation, water purification, and industrial distillation. Important measures of how effective membranes are include: molecular weight cut-off, or particle rejection, and flux of fluid through a membrane. Many conventional membranes have cylindrical pores, which have a circular surface area on the surface of particle interaction. Therefore, when making these cylindrical pore membranes, there is only one length scale to manipulate particle cut off and flux through the membrane. However, slit-like pores, also known as elliptical or elongated pores, have two length scales to manipulate which provides more control over cut off and flux through the membrane. These two length scales are the major and minor axis, or length and width, of the slit-like ellipse. For a given area, a slit-like pore has a higher cut-off, or greater selectivity, since it can reject smaller sized particles due to the smaller dimension of the minor axis in comparison to the single length scale of a cylindrical pore [7]. The RM257/5CB mixture is promising for applications in membrane particle filtration. However, the optimum ratio of RM257/5CB and the physical properties of this mixture are unknown.

One objective of this research is to maximize aspect ratio, the division of length versus width (r_x/r_y) of the slit-like pore. When aspect ratio (AR) increases, membrane flux also increases due to the elongated length of the pore and the shorter width of the pore. One goal of this research would be to create pore widths as small as 10nm to reject virus particles.

Methods

Functionalized PI-Coated Glass Procedure

Polyimide (PI) coated glass slides are necessary for LC planar anchoring [2]. To make this functionalized glass, first gather polyimide (PI2555) from fridge and thinner (T9039) from flammable storage cabinet and let them sit out for 1 hour without opening so that they can reach room temperature without adsorbing moisture. Then make 1:10 PI:thinner dilution. Note: polyvinyl alcohol (PVA) can be used in place of polyimide [2]. Set oven to 250 °C. Cut slides into a 48X48 mm square to fit into spin coater. Place glass slides in a glass beaker where they won't lay on top of each other and fill with mQ water andalconox detergent. Place in sonicator for 10 minutes. Rinse detergent off glass slides with mQ water. Remove glass slides one-by-one, drying with air, blowing in same direction one edge to the other and holding by corners to not leave marks. After drying, put glass in oven at 250 °C for a few seconds to evaporate excess moisture. Drop 6-7 drops of PI:thinner solution onto slides using a syringe until most of the glass is covered. Turn on spin coater for 10 seconds at 1000 rpm and then 30 seconds for 3000 rpm. Place slides in oven for 2 hours at 250 °C. After 2 hours, turn off oven and let it cool to room temperature before removing and storing slides. To keep track of the PI coated side, mark small dots on two corners of the slide on the non-coated side with permanent marker.

Membrane Manufacturing Procedure

Mix the intended molar ratio of RM257/5CB + 2 wt% (with respect to RM257) photoinitiator (1-hydroxycyclohexyl phenyl ketone) in a glass vial. Place the glass vial in the oven at 100 °C for an hour, until the mixture is fully melted. Momentarily mix with the vortex. Set oven to 80 °C. Rub PI-coated glass with sandpaper for a few strokes. This ensures that the surface will have uniform planar alignment [2]. Make a sandwich cell of rubbed PI coated glasses in a way that the rubbing directions are parallel to each other and perpendicular to the open sides of the sandwich cell. Set the hot plate at the intended relative temperature for crosslinking as provided by Hopwood's equation 1 [8].

$$T_{crosslink} = [(T_{NB} + 273.15) * T_{rel}] - 273.15 \quad (1)$$

Where $T_{crosslink}$ is the crosslinking temperature in Celsius, T_{rel} is the desired relative temperature, and $T_{NB} = 1.0711(mol\% RM257) + 47.748$ as provide in Appendix Figure A1 [8]. Determining the desired $T_{crosslink}$ is out of the scope of this paper but is something that will need to be further investigated. See Appendix Figure A1. for the phase transition diagram for various RM257/5CB concentrations. Inject 200-400 μ L (depending on the size of the membrane) to the sandwich cell while the sandwich cell is placed on the hot plate. Turn the ultraviolet light on, with a wavelength setting of 365 nm, while the membrane is enclosed in a dark environment and let it cure in the light for 30 minutes. After crosslinking, immediately transfer the cell to the oven at 80 °C for 15 minutes. Let the cell cool to room temperature, then place sandwiched membrane in an ethanol bath for a few hours. Remove membrane from sandwich using a razor blade. Store the membrane in water.

SEM Nova Sample Preparation and Image Analysis

Prepare a sample by cutting the membrane with scissors to a sufficient size and taping it with SEM nonconductive adhesive tabs to a mount used within the SEM. Use the sputter coater to coat the sample in gold for 120 seconds. Use SEM Nova to take images of the sample to analyze membrane morphology. Use ImageJ to measure the length and width of the pores. Calculate AR of each pore.

Results

Using the SEM Nova, images were taken for 9.8, 15, 20, and 25 mol% RM257 membranes. The 9.8 and 15 mol% RM257 appeared to contain slit-like pores, as shown in Figure 3. The results from 20 and 25 mol% were not as clear. AR calculations were interpreted from Figure 3 to produce Figure 4. From Figure 4(a), as mol% of RM257 increases, so does the AR, or r_x/r_y . This means that for RM257 concentrations between about 10-15 mol%, pores become more slit-like. From Figure 4(b), as mol% of RM257 increases, so does length, r_x for the same 10-15mol% range.

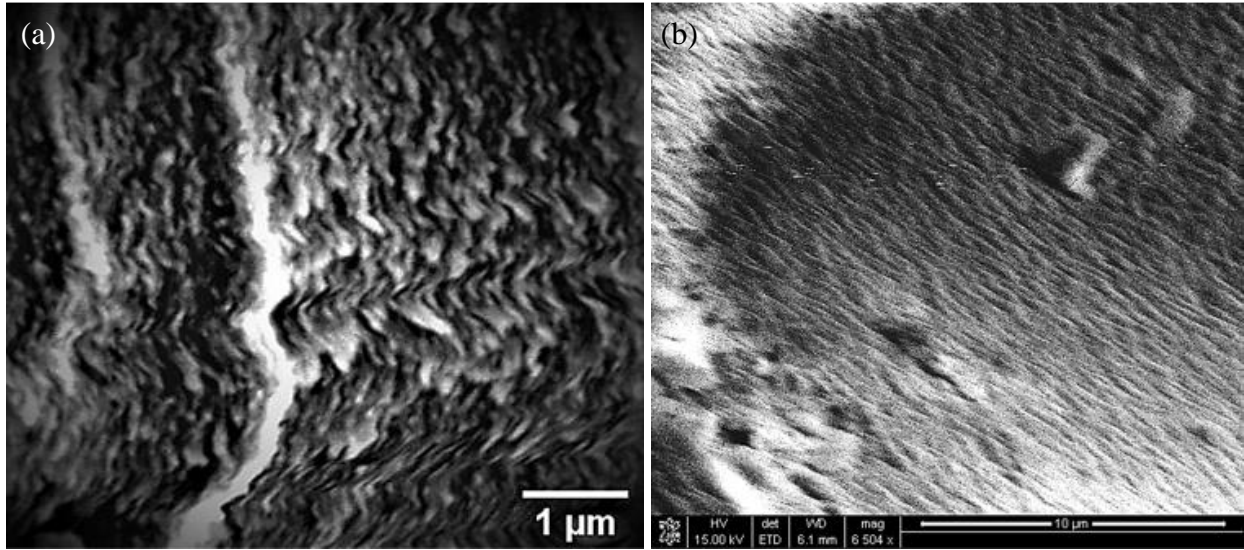


Figure 3. SEM membrane images of (a) 9.6 mol% RM257 and (b) 15 mol% RM257

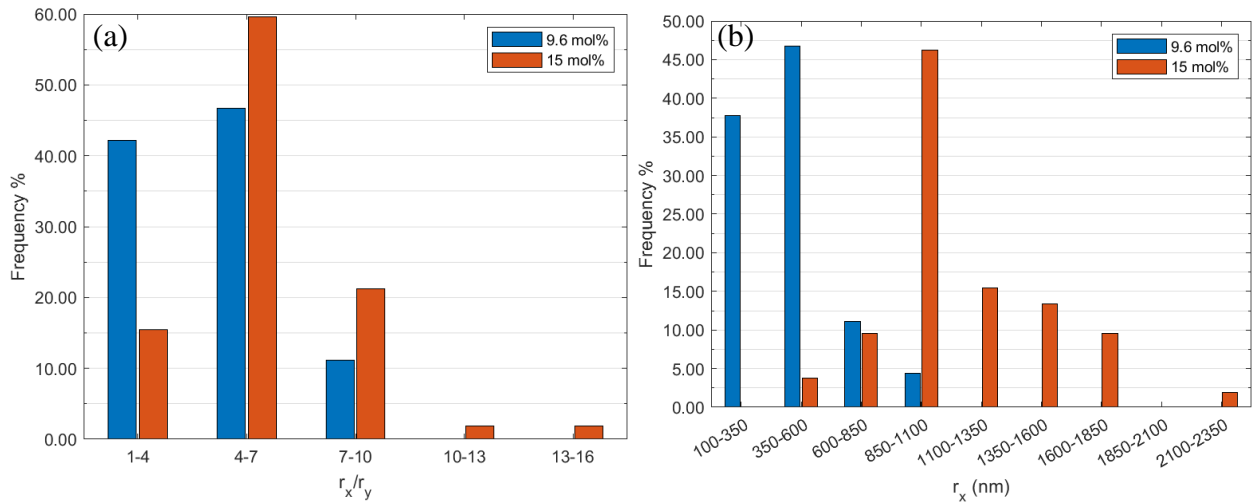


Figure 4. For 9.6 and 15 mol% RM257 (a) AR versus frequency and (b) length versus frequency

A paired two-sample for means t-test was performed to ascertain if the null hypothesis (AR means of two membranes are equal) can be accepted or rejected. The t-test results are shown in Table 1 below. The p-value for a two-tailed t-test was 6.50×10^{-12} which is smaller than $\alpha = 0.05$, so the null hypothesis can be rejected. Also, since t-stat, 9.34, is greater than t-critical, 2.02, that also concludes that the null hypothesis can be rejected. Therefore, there is sufficient evidence to say that the ARs of the two membranes are statistically significant.

Table 1. 2-sample t-test results of AR for 9.6 and 15 mol% RM257 membranes

| | <i>AR 9.6mol%</i> | <i>AR 15mol%</i> |
|------------------------------|-------------------|------------------|
| Mean | 4.81 | 6.01 |
| Variance | 2.27 | 4.89 |
| Observations | 44 | 44 |
| Hypothesized Mean Difference | 0 | |
| Degrees of Freedom | 43 | |
| t Stat | 9.34 | |
| P(T<=t) two-tail | 6.50E-12 | |
| t Critical two-tail | 2.02 | |

To further compare the two membranes, the ranges of AR, length, and width will be discussed and are also displayed in Table 2 below.

1. For the 9.6 mol% RM257 membrane, the AR ranged from 1.95-9.06 while the 15 mol% membrane AR ranged from 2.0-14.09. For the 9.6 mol% RM257 membrane, the average AR was 4.75 while the 15 mol% membrane average AR was 5.89. Therefore, as mol% of RM257 increased from 9.6 to 15 mol%, AR increased by about 1.14.
2. For the 9.6 mol% RM257 membrane, the length ranged from 165.48-1,047.15 nm while the 15 mol% membrane length ranged from 529.87-2,281.46 nm. For the 9.6 mol% RM257 membrane, the average length was 458.04 while the 15 mol% membrane average length was 1138.63. Therefore, as mol% of RM257 increased from 9.6 to 15 mol%, length increased by about 681 nm.
3. For the 9.6 mol% RM257 membrane, the width ranged from 39.93-256.64 nm while the 15 mol% membrane width ranged from 109.83-396.03 nm. For the 9.6 mol% RM257 membrane, the average width was 104.49 while the 15 mol% membrane average width was 207.72. Therefore, as mol% of RM257 increased from 9.6 to 15 mol%, width increased by about 103 nm.

Table 2. Measurement results for 9.6 and 15 mol% RM257 membranes

| | 9.6 mol% RM257 | 15 mol% RM257 |
|----------------|-------------------|-------------------|
| Width Range | 39.93 - 256.64 | 109.83 - 396.03 |
| Average Width | 104.49 | 207.72 |
| Length Range | 165.48 - 1,047.15 | 529.87 - 2,281.46 |
| Average Length | 458.04 | 1138.63 |
| AR Range | 1.95 - 9.06 | 2.0 - 14.09 |
| Average AR | 4.75 | 5.89 |

When looking at higher concentrated mixtures, with respect to RM257, the slit-like pore morphology dissipated. Figure 5(a) suggests a more cylindrical pore morphology at 20 mol% RM257. Figure 5(b) does not even share the same morphology as any of the lower mol% RM257 membranes and instead displays larger pores. More analysis is needed to deduce firm conclusions of membrane morphology above 15 mol% RM257.

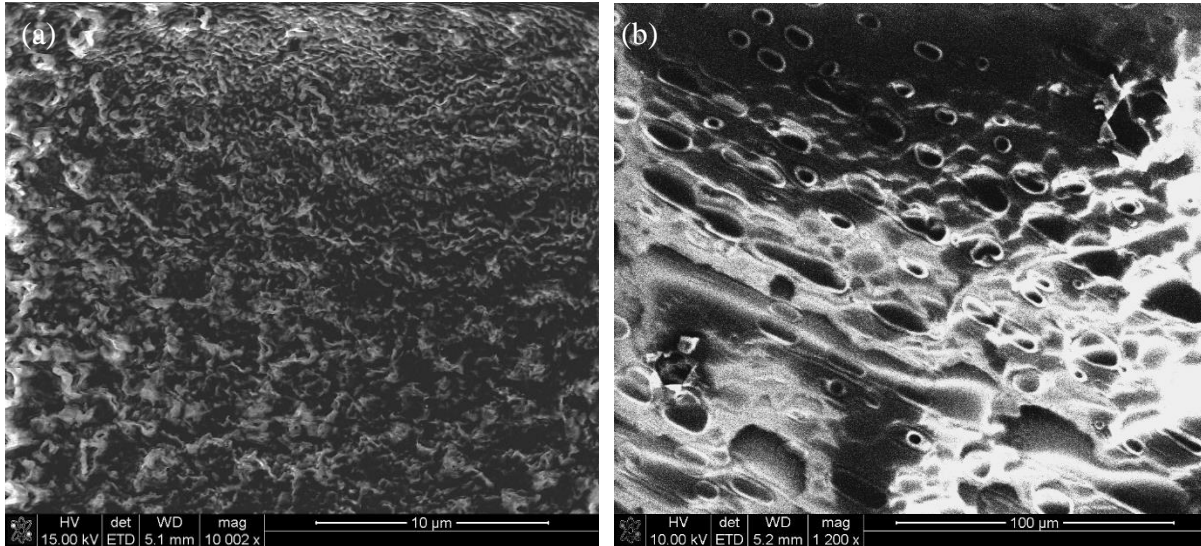


Figure 5. SEM membrane images of (a) 20 mol% RM257 and (b) 25 mol% RM257

Conclusion and Future Work

The purpose of this research is to manufacture a membrane with slit-like pores to achieve particle filtration. Slit-like pore membranes are preferred over conventional membranes that contain cylindrical pores. Between 9.8-15 mol% of RM257, the aspect ratio increased, meaning the pores became more slit-like. Likewise, as mol% of RM257 increased from 9.8-15 mol%, so did the length of the pore. There is sufficient evidence to say that the ARs of the 9.8 and 15 mol% membranes are statistically significant. Membranes with 20 and 25 mol% RM257 did not display slit-like pore morphology.

In the future, more data needs to be collected from samples with different concentrations of RM257 for pore size analysis. Also, crosslinking at different relative temperatures is necessary to find the best temperature at which the membrane's physical properties are optimum. Glass transition temperature, by using differential scanning calorimetry, should also be investigated to help find with the study of membrane properties. Filtration studies to find membrane energy efficiency, mechanical properties, and the rejection rate for virus rejection application should also be conducted.

Acknowledgments

Thank you to all those who have helped with this project including Dr. Nayani, Isaac Hopwood, Homa Ghaiedi, and Jude Obijiaku. I would also like to acknowledge the Ralph E. Martin Department of Chemical Engineering Department and the University of Arkansas Honors College.

References

- [1] S. Oladepo, “Temperature-dependent fluorescence emission of 4-cyano-4'-pentylbiphenyl and 4-cyano-4'-hexylbiphenyl liquid crystals and their bulk phase transitions,” *J. Mol. Liq.*, vol. 323, p. 114590, Oct. 2020, doi: 10.1016/j.molliq.2020.114590.
- [2] A. Karausta and E. Bukusoglu, “Liquid Crystal-Templated Synthesis of Mesoporous Membranes with Predetermined Pore Alignment,” *ACS Appl. Mater. Interfaces*, vol. 10, no. 39, pp. 33484–33492, Oct. 2018, doi: 10.1021/acsami.8b14121.
- [3] J. Pavlin, N. Vaupotic, and M. Čepič, “Liquid crystals: a new topic in physics for undergraduates,” *Eur. J. Phys.*, vol. 34, Nov. 2012, doi: 10.1088/0143-0807/34/3/745.
- [4] E. Bukusoglu, M. Bedolla Pantoja, P. C. Mushenheim, X. Wang, and N. L. Abbott, “Design of Responsive and Active (Soft) Materials Using Liquid Crystals,” *Annu. Rev. Chem. Biomol. Eng.*, vol. 7, no. 1, pp. 163–196, 2016, doi: 10.1146/annurev-chembioeng-061114-123323.
- [5] J.-L. Zhu *et al.*, “Improved Kerr constant and response time of polymer-stabilized blue phase liquid crystal with a reactive diluent,” *Appl. Phys. Lett.*, vol. 102, Feb. 2013, doi: 10.1063/1.4793416.
- [6] J.-H. Lee, T. Kamal, S. V. Roth, P. Zhang, and S.-Y. Park, “Structures and alignment of anisotropic liquid crystal particles in a liquid crystal cell,” *RSC Adv.*, vol. 4, no. 76, pp. 40617–40625, 2014, doi: 10.1039/C4RA06221C.
- [7] B. J. Feinberg, J. C. Hsiao, J. Park, A. L. Zydney, W. H. Fissell, and S. Roy, “Slit pores preferred over cylindrical pores for high selectivity in biomolecular filtration,” *J. Colloid Interface Sci.*, vol. 517, pp. 176–181, May 2018, doi: 10.1016/j.jcis.2017.12.056.
- [8] Hopwood, Isaac, “Synthesis and Phase Transition Characterization of Liquid Crystal Membranes with Slit-Like Pores,” Apr. 2022.

Appendix

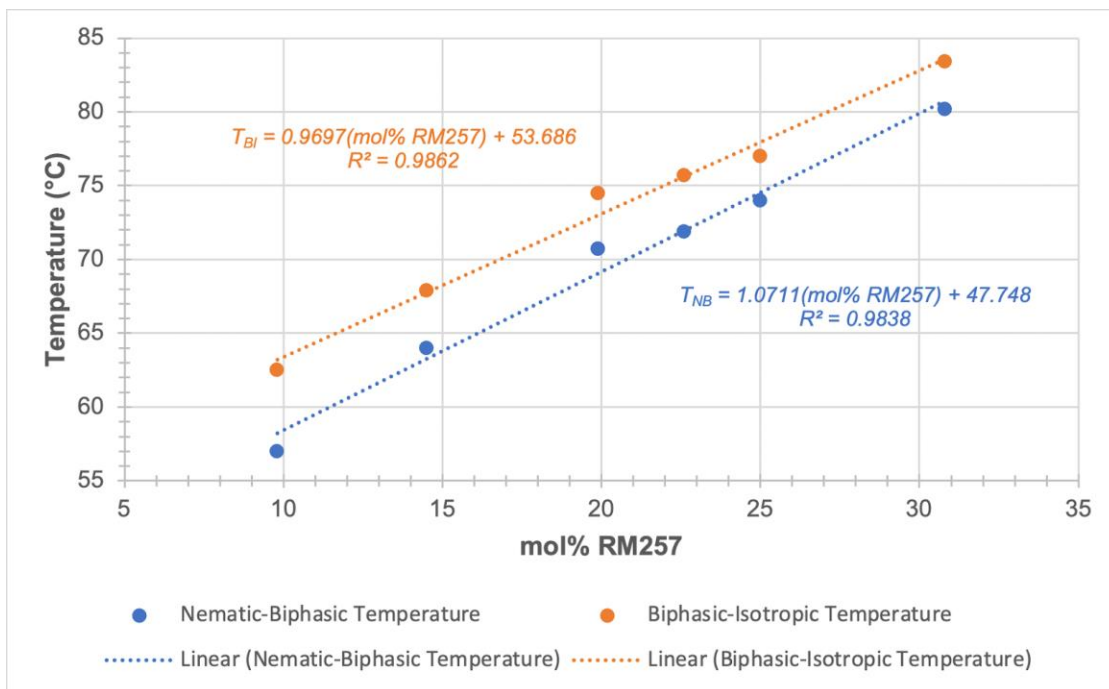


Figure A1. RM257/5CB phase transition diagram [8]